Synthesis and Photochemistry of Amido-Linked, Peripherally-Molybdenated Tetraphenylporphyrins

Natalie M. Rowley,* Stefan S. Kurek, Peter R. Ashton, Tom A. Hamor, Christopher J. Jones, and Neil Spencer

School of Chemistry, University of Birmingham, Edgbaston, Birmingham B15 2TT, U.K.

Jon A. McCleverty*

School of Chemistry, University of Bristol, Cantocks Close, Bristol BS8 1TS, U.K.

Godfrey S. Beddard,† Timothy M. Feehan, and Nigel T. H. White

Department of Chemistry, University of Manchester, Oxford Road, Manchester, M13 9PL, U.K.

Eric J. L. McInnes, Nicholas N. Payne, and Lesley J. Yellowlees

Department of Chemistry, University of Edinburgh, Edinburgh EH9 3JJ, U.K.

Received July 27, 1995[⊗]

The *para*, *meta*, and *ortho* peripherally-molybdenated tetraphenylporphyrin complexes [5-{[Mo(NO)Tp*Cl]-NHC_6H_4}-10,15,20-Ph_3porphH_2] [**1**−**3**, respectively; Tp* = hydrotris(3,5-dimethylpyrazol-1-yl)borate; Ph_3porphH_2 = triphenylporphyrin] have been prepared by reaction of the corresponding 5-(aminophenyl)-10,15,20-triphenylporphyrin derivative with [Mo(NO)Tp*Cl_2]. Cyclic voltammetry shows that most of these complexes undergo two oxidation processes (associated with the porphyrin) and three reduction processes (two associated with the porphyrin, and one with the molybdenum fragment). The redox potentials of the molybdenum fragment are little influenced by the presence of the macrocyclic ring, and *vice versa*. The $\Delta G°$ values for charge separation in **1**−**3** are close to 0 eV. Photochemical measurements have been made on **1**−**3**, and they were all found to undergo photoinduced intramolecular electron transfer from the excited singlet state of the porphyrin macrocycle to the molybdenum moiety, yielding charge-separated states with lifetimes of 300−340 ps. Further studies, using electrochemical methods and EPR spectroscopy, have been made to investigate the nature of the reduced molybdenum species. The molecular structure of **3** was determined crystallographically: $C_{59}H_{52}N_{12}BClMoO$, monoclinic, space group $P2_1/c$, a = 13.678(6), b = 16.650(2), and c = 26.555(6) Å, β = 91.56(3)°, Z = 4. It was shown that the Mo−NH (aniline) distance is relatively short [1.928(16) Å], consistent with $p_\pi \rightarrow d_\pi$ donation. The Mo−porphyrin centroid distance is 6.75 Å.

Introduction

Despite the many reported examples of intramolecular electron transfer from porphyrin to organic acceptors such as quinone, methyl viologen, and pyromellitimide,[1] and the abundance of metalloporphyrin complexes in which the porphyrin acts as a macrocyclic ligand,[2,3] examples of electron transfer to externally- but covalently-linked transition metal-based redox centers are very rare. Our original interest in making [5-{[Mo(NO)Tp*Cl]EC_6H_4}-10, 15, 20-Ph_3porphH_2] (E = O, NH) stemmed from a desire to make a study in which a redox-active transition metal is used as an electron-acceptor moiety in a photoactive system. The reduction potential of the transition metal can then be varied, enabling the subsequent effect upon the rate of electron transfer to be assessed. In a previous paper, we described complexes in which the electron-withdrawing [Mo(NO)Tp*Cl] group [Tp* = tris(3,5-dimethylpyrazolyl)borate, HB(3,5-$Me_2C_3HN_2)_3$] was attached to the periphery of a tetraphenylporphyrin ring via *para*, *meta*, and *ortho* phenolic links, this forming the first part of our study.[4] We have shown that there is no significant influence of the molybdenum center on the porphyrin ring (or *vice versa*) in the ground state, although part of the Tp* ligand approaches the porphyrin ring in [5-{*o*-([Mo(NO)Tp*Cl]O)C_6H_4}-10,15,20-Ph_3porphH_2] quite closely. Species of the type [5-{[Mo(NO)-Tp*Cl]OC_6H_4}-10,15,20-Ph_3porphH_2] exhibit luminescence quenching,[5] and this was found to be the result of electron transfer from the excited singlet state of the porphyrin to the [Mo(NO)Tp*Cl] moiety, the LUMO of the molybdenum-

† Present address: School of Chemistry, University of Leeds, Leeds LS2 9JT, U.K.

⊗ Abstract published in *Advance ACS Abstracts,* November 15, 1996.

(1) Fox, M. A.; Chanon, M. *Photoinduced Electron Transfer;* Elsevier: Amsterdam, 1988; Part D, Chapter 6.2.

(2) Morgan, B.; Dolphin, D. *Struct. Bonding* **1987**, *64*, 116−203. Hamilton, A. D.; Rubin, H.-D.; Bocarsly, A. B. *J. Am. Chem. Soc*. **1984**, *106*, 7255−7257.

(3) Montanari, F., Casella, L., Eds. *Metalloporphyrins Catalysed Oxidations*; Kluwer Academic Publications: Dordrecht, The Netherlands, 1994; pp 49−86.

(4) Rowley, N. M.; Kurek, S. S.; Foulon, J.-D.; Hamor, T. A.; Jones, C. J.; McCleverty, J. A.; Hubig, S. M.; McInnes, E. J. L.; Payne, N. N.; Yellowlees, L. J. *Inorg. Chem.* **1995**, *34*, 4414−4426.

(5) Rowley, N. M.; Kurek, S. S.; George, M. W.; Hubig, S. M.; Beer, P. D.; Jones, C. J.; Kelly, J. M.; McCleverty, J. A. *J. Chem. Soc., Chem. Commun*. **1992**, 497−499.

S0020-1669(95)00934-7 CCC: $12.00

acceptor center being energetically accessible to the excited singlet state of the porphyrin donor.

This second part of our study focuses on complexes of the type [5-{[Mo(NO)Tp*Cl]NHC$_6$H$_4$}-10,15,20-Ph$_3$porphH$_2$]. Amido complexes, formally isoelectronic with phenolic species of the type [Mo(NO)Tp*X(OAr)] (X = halide), are readily prepared by the reaction of [Mo(NO)Tp*X$_2$] with anilines,[6] but, in contrast, the redox potential of the molybdenum centers is substantially cathodically shifted, reducing at *ca*. −0.76 V, which is approximately the same energy as that of the excited singlet state of the porphyrin. The $\Delta G°$ values for charge separation are, therefore, close to 0 eV in species of the type [5-{[Mo(NO)Tp*Cl]NHC$_6$H$_4$}-10,15,20-Ph$_3$porphH$_2$]. Nevertheless, these complexes were found to exhibit luminescence quenching, analogous to that observed with [5-{[Mo(NO)Tp*Cl]-OC$_6$H$_4$}-10,15,20-Ph$_3$porphH$_2$].[5]

In this paper, we report the characterization of *para*, *meta*, and *ortho* complexes [5-{[Mo(NO)Tp*Cl]NHC$_6$H$_4$}-10,15,20-Ph$_3$porphH$_2$] (**1**−**3**, respectively), synthesized by reaction of [Mo(NO)Tp*Cl$_2$] with the appropriate mono(aminophenyl)-triphenylporphyrins. The electrochemical and photochemical properties of these new complexes and the molecular structure of **3** have also been determined. We have also used spectroelectrochemical techniques (for example, examination of the EPR spectra of [**1**]$^-$) to support our view that the LUMO on the molybdenum center is the ultimate receptor for the phototransferred electron.

Experimental Section

General Details. All reactions were carried out under an oxygen-free, dry nitrogen atmosphere. Dry, freshly distilled toluene was used for all reactions. Triethylamine was dried over sodium. The starting material [Mo(NO)Tp*Cl$_2$] was prepared according to known procedures.[7] [(*p*-, [(*m*-, and [(*o*-NO$_2$C$_6$H$_4$)Ph$_3$porphH$_2$] and [(*p*-, [(*m*-, and [(*o*-NH$_2$C$_6$H$_4$)Ph$_3$porphH$_2$] were prepared as described in the literature.[8,9] New compounds were purified by column chromatography (column lengths *ca*. 0.3 m) using Kiesel gel 60 (Merck, 70−230 mesh). IR spectra were recorded with a PE297 spectrophotometer using KBr disks. ^{1}H NMR spectra were recorded using a JEOL GX-270 (270 MHz) spectrometer, a Bruker AC300 (300 MHz), or a Bruker AMX400 (400 MHz) spectrometer. NOE measurements were made using standard Bruker software *via* a phase-sensitive 2D-NOESY experiment performed with a mixing time of 300 ms. Low-resolution liquid secondary ion mass spectra (LSIMS) were obtained from a VG Zabspec mass spectrometer, utilizing a *m*-nitrobenzyl alcohol matrix and scanning in the positive ion mode at a speed of 5 s/decade. High-resolution accurate mass measurements (HRLSIMS) were obtained by operating at a resolution of 6000 and employing narrow-range voltage scanning with poly(ethylene glycol) as a reference. Absorption spectra were obtained using a Shimadzu UV-240 spectrophotometer.

Femtosecond transient absorption measurements were carried out using a pump−probe system based on a colliding pulse mode-locked laser, a pulse from which was amplified to 500 μJ at 10 Hz by a Nd/YAG laser. Part of this pulse (duration, 150 fs fwhm) was used to generate a continuum for use as the probe pulse; the remainder was the pump. The excitation wavelength was 620 nm for all experiments. Quoted lifetimes and rate constants have an expected accuracy of ±10%.

Cyclic voltammetry was carried out using an EG & G Model 174A polarographic analyzer, with *ca*. 10^{-3} mol dm^{-3} solutions under dry N_2 in dry dichloromethane. A Pt bead working electrode was used, with 0.2 mol dm^{-3} [*n*-Bu$_4$N][BF$_4$] as supporting electrolyte and a scan rate of 200 mV s^{-1}. Potentials were recorded *vs* a saturated calomel reference electrode, and ferrocene was added as an internal standard. The data obtained were reproducible, the experimental error being ±10 mV. All spectroelectrochemical studies were carried out using an Autolab System containing a PSTAT10 potentiostat, using General Purpose Electrochemical System (GPES) Version 3 software, linked to a Hewlett-Packard 7045A *X*−*Y* recorder. Positive feedback ohmic compensation was applied for all cyclic voltammograms recorded. Cells were thermostated using a Haake Model Q thermostated bath circulator. Coulometric experiments utilized an H-type cell with the Pt basket working electrode fritted from the Pt counter electrode. Inert electrolyte, [*n*-Bu$_4$N][BF$_4$], was used in 0.5 mol dm^{-3} concentration in CH_2Cl_2. All solutions were purged with Ar for 20 min prior to study. Electrogeneration potentials were 150 mV more positive than the E_f for the couple.

The optically transparent electrode cell (OTE) for use in UV/vis/near-IR spectrometers has been described previously.[10] EPR spectra were recorded on an X-band Bruker ER200D-SCR spectrometer.

Microanalyses were performed by the Microanalytical Laboratory of the School of Chemistry in the University of Birmingham.

Preparation of Complexes 1−3. To a solution of the appropriate isomer of [(H$_2$NC$_6$H$_4$)Ph$_3$porphH$_2$] (0.06 g, 0.10 mmol) and [Mo(NO)-Tp*Cl$_2$] (0.05 g, 0.10 mmol) in dry toluene (50 cm^3) was added NEt$_3$ (0.2 cm^3), and the mixture was refluxed for 3.5 h. *n*-Pentane (20 cm^3) was added to the cooled solution, and the mixture was then kept in a refrigerator overnight. The ammonium salts that had precipitated were filtered off, and the solvent was then removed *in vacuo*. The residue was chromatographed on silica gel using a mixture of dichloromethane and *n*-hexane (1:1 v/v) as eluant. The main brown fraction was collected, the solvent removed *in vacuo*, and the desired product obtained as purple crystals by recrystallization from dichloromethane/*n*-hexane.

1: yield 0.06 g (59%); ^{1}H NMR (270 MHz, CDCl$_3$) δ 12.96 (1H, s, N*H*C$_6$H$_4$), 8.93 (4H, A$_2$B$_2$, J_{AB} = 4.8 Hz, $\Delta\delta_{AB}$ = 0.1 ppm, pyrrole protons of rings A and B), 8.85 (4H, s, pyrrole protons of rings C and D), 8.29 (2H, d, $J_{pp'}$ = 8.4 Hz, H$_p$ and H$_{p'}$ of NHC$_6$*H*$_4$porphH$_2$), 8.22 (6H, m, *ortho* protons of Ph in Ph$_3$porphH$_2$), 7.88 (2H, d, $J_{qq'}$ = 8.4 Hz, H$_q$ and H$_{q'}$ of NHC$_6$*H*$_4$porphH$_2$), 7.76 (9H, m, *meta* and *para* protons of Ph in Ph$_3$porphH$_2$), 5.96 (1H, s), 5.92 (1H, s), 5.91 (1H, s, Me$_2$C$_3$*H*N$_2$), 2.77 (3H, s), 2.62 (3H, s), 2.47 (3H, s), 2.43 (3H, s), 2.41 (3H, s), 2.35 (3H, s, (C*H*$_3$)$_2$C$_3$HN$_2$), −2.73 (2H, s, central N*H* of porphyrin ring); LSIMS *m/z* 1088 (M$^+$), 630 [(H$_2$NC$_6$H$_4$)Ph$_3$porphH$_2^+$]; IR (KBr disk) 3310w, 3285w (±10, ν_{NH}), 2920w, 2845w (±10, ν_{CH}), 2545w (±10, ν_{BH}), 1660s, 1650sh (±5, ν_{NO}), 1535m (±5, $\nu_{C=C}$), 1435s, 1415s, 1378s, 1362s (±5, ν_{C-Me}) cm^{-1}. Anal. Calcd for C$_{59}$H$_{52}$N$_{12}$BClMoO: C, 65.2; H, 4.8; N, 15.5. Found: C, 65.6; H, 4.8; N, 15.1.

2: yield 0.04 g (32%); ^{1}H NMR (300 MHz, CDCl$_3$) δ 12.87 (1H, s, N*H*C$_6$H$_4$), 8.90 (AB, unresolved), 8.84 (8H, s, pyrrole protons of rings A, B, C, and D), 8.33 (1H, d, J = 9.5 Hz, H$_q$/H$_s$ of NHC$_6$*H*$_4$porphH$_2$), 8.20 (6H, m, *ortho* protons of Ph in Ph$_3$porphH$_2$), 8.05 (1H, d, J = 7.5 Hz, H$_q$/H$_s$ of NHC$_6$*H*$_4$porphH$_2$), 7.93 (1H, s, H$_p$ of NHC$_6$*H*$_4$porphH$_2$), 7.88 (1H, dd, $J \approx$ 7.8 Hz, H$_r$ of NHC$_6$*H*$_4$porphH$_2$), 7.75 (9H, m, *meta* and *para* protons of Ph in Ph$_3$porphH$_2$), 5.88 (1H, s), 5.86 (1H, s), 5.81 (1H, s, Me$_2$C$_3$*H*N$_2$), 2.69 (3H, s), 2.49 (3H, s), 2.40 (3H, s), 2.34 (9H, s, (C*H*$_3$)$_2$C$_3$HN$_2$), −2.77 (2H, s, central N*H* of porphyrin ring). LSIMS *m/z* 1088 (M$^+$), 630 [(H$_2$NC$_6$H$_4$)Ph$_3$porphH$_2^+$]; HRLSIMS found (M$^+$) 1088.3180, C$_{59}$H$_{52}$N$_{12}$BClMoO requires 1088.3223; IR data

(6) (a) Jones, C. J.; McCleverty, J. A.; Neaves, B. D.; Reynolds, S. J.; Adams, H.; Bailey, N. A.; Denti, G. *J. Chem. Soc., Dalton Trans.* **1986**, 733−741. (b) Al Obaidi, N.; Charsley, S. M.; Hussain, W.; Jones, C. J.; McCleverty, J. A.; Neaves B. D.; Reynolds, S. J. *Transition Met. Chem.* **1987**, *12*, 143−148.

(7) Reynolds, S. J.; Smith, C. F.; Jones, C. J.; McCleverty, J. A. *Inorg. Synth.* **1985**, *23*, 4−9.

(8) Adler, A. D.; Longo, F. R.; Finarelli, J. D.; Goldmacher, J.; Assour, J.; Korsakoff, L. *J. Org. Chem.* **1967**, *32*, 476. Adler, A. D.; Longo, F. R.; Shergalis, W. *J. Am. Chem. Soc.* **1964**, *86*, 3145−3149. Although not used in this work, more recently an improved method has been published: Semeikin, A. S.; Koifman, O. I.; Berezin, B. D. *Khim. Geterotsikl. Soedin.* **1982**, 1354−1355.

(9) Collman, J. P.; Brauman, J. I.; Doxsee, K. M.; Halbert, T. R.; Bunnenberg, E.; Linder, R. E.; LaMar, G. N.; Del Gaudio, J.; Lang, G.; Spartalian, K. *J. Am. Chem. Soc.* **1980**, *102*, 4182−4192.

(10) Macgregor, S. A.; McInnes, E.; Sorbie, R. J.; Yellowlees, L. J. In *Molecular Electrochemistry of Inorganic, Bioinorganic and Organometallic Compounds*; Pombeiro, A. J. L., McCleverty, J. A., Eds.; Kluwer Academic Publishers: Dordrecht, The Netherlands, 1993; pp 503−517.

Table 1. Structural Studies of **3**

chemical formula	$C_{59}H_{52}N_{12}BClMoO$	formula weight	1087.4
		space group	$P2_1/c$ (No. 14)
a	13.678(6) Å	T	20 °C
b	16.650(2) Å	λ	0.71069 Å
c	26.555(6) Å	ρcalc	1.20 g cm^{-3}
β	91.56(3)°	μ (Mo Kα)	3.00 cm^{-1}
V	6045 Å^3	$R(F_o)^a$	0.090
Z	4	$R_w(F_o)^b$	0.095

^{a} $R(F_o) = \sum(|F_o| - |F_c|)/\sum|F_o|$. ^{b} $R_w(F_o) = [\sum w(|F_o| - |F_c|)^2/\sum w|F_o|^2]^{1/2}$.

(KBr disk) 3310w, 3278w (±10, ν_{NH}), 2920w, 2850w (±10, ν_{CH}), 2545w (±10, ν_{BH}), 1660s, 1650sh (±5, ν_{NO}), 1532m (±5, $\nu_{C=C}$), 1438s, 1410s, 1378s, 1362s (±5, ν_{C-Me}) cm^{-1}. Anal. Calcd for $C_{59}H_{52}N_{12}BClMoO$: C, 65.2; H, 4.8; N, 15.5. Found: C, 64.7; H, 5.2; N, 14.9.

3: yield 0.05 g (49%); ^{1}H NMR (300 MHz, $CDCl_3$) δ 12.30 (1H, s, N*H*C_6H_4), 8.87 (2H, s, pyrrole protons of rings C and D), 8.82 (3H, m, H_p/H_s of NHC$_6H_4$porphH$_2$ and pyrrole protons of rings C and D), 8.72 (2H, AB, $J_{AB} \approx 4.8$ Hz, $\Delta\delta_{AB} = 0.1$ ppm, $H_{a'}$,$H_{b'}$ or H_a,H_b, pyrrole protons of rings A and B), 8.49 (2H, AB, $J_{AB} \approx 4.8$ Hz, $\Delta\delta_{AB} = 0.1$ ppm, $H_{a'}$,$H_{b'}$ or H_a,H_b, pyrrole protons of rings A and B), 8.27−8.05 (6H, m, *ortho* protons of Ph in Ph$_3$porphH$_2$), 8.12 (1H, d, $J \approx 7.5$, 1.5 Hz, H_p/H_s of NHC$_6H_4$porphH$_2$), 8.00 (1H, dd, $J \approx 8.3$, 1.5 Hz H_q/H_r of NHC$_6H_4$porphH$_2$), 7.78 (9H, m, *meta* and *para* protons of Ph in Ph$_3$porphH$_2$), 7.58 (1H, dd, $J \approx 7.4$, 1.0 Hz, H_q/H_r of NHC$_6H_4$porphH$_2$), 5.62 (1H, s), 5.60 (1H, s), 2.82 (1H, s) (Me$_2$C$_3H$N$_2$), 2.52 (3H, s), 2.46 (3H, s), 1.96 (3H, s), 1.85 (3H, s), 0.93 (3H, s), 0.52 (3H, s, (CH_3)$_2$C$_3$HN$_2$), −2.92 (2H, s, central N*H* of porphyrin ring); LSIMS *m/z* 1088 (M$^+$), 630 [(H$_2$NC$_6$H$_4$)Ph$_3$porphH$_2^+$]; HRLSIMS found (M$^+$) 1088.3264, $C_{59}H_{52}N_{12}BClMoO$ requires 1088.3223; IR data (KBr disk) 3310w, 3245w (±10, ν_{NH}), 2918w, 2840w (±10; ν_{CH}), 2530w (±10, ν_{BH}), 1652s (±5, ν_{NO}), 1535m (±5, $\nu_{C=C}$), 1438s, 1410s, 1375s, 1360s (±5, ν_{C-Me}) cm^{-1}. Anal. Calcd for $C_{59}H_{52}N_{12}BClMoO(C_6H_{14})$: C, 66.5; H, 5.7; N, 14.3. Found: C, 66.5; H, 5.4; N, 14.2.

Structure Determination of 3. Dark purple crystals of **3** were grown from CH_2Cl_2/*n*-hexane. The crystals were platelike in shape. Data were collected using an Enraf-Nonius CAD-4 diffractometer equipped with a graphite monochromator. Cell dimensions and intensities were measured by $\omega/2\theta$ scans. A total of 8384 reflections were scanned in the range $2 < \theta < 23°$, with $-15 < h < 15$, $-1 < k < 18$, and $-1 < l < 29$, and of these, 2823 unique reflections having $I > 2.5\sigma(I)$ were considered observed and were used for the structure solution and refinement. Three standard reflections measured every 2 h showed no significant variation in intensity. The structure was solved by the conventional heavy-atom method, and successive difference Fourier syntheses were used to locate all non-hydrogen atoms, followed by final refinements using full-matrix least-squares procedures. Hydrogen atoms were placed in calculated positions riding on their respective bonded atoms, except for the imino hydrogen atoms, which were not included. Refinement converged at $R = 0.090$ ($R_w = 0.095$). The final electron density difference synthesis showed no peaks greater than +1.0 or less than −0.5 e Å^{-3}. Crystal data are given in Table 1, and the final atomic coordinates are listed in Table 2. Estimated standard deviations are relatively large due to the poor quality of the crystals, resulting in a paucity of data. Computations were performed on the University of Birmingham IBM 3090 computer with the SHELXS 86,[11] SHELX 76,[12] and DIFFABS[13] packages. The molecular diagram was drawn using ORTEP.[14] Scattering factors with corrections for anomalous dispersion were taken from *International Tables for X-Ray Crystallography*.[15] All non-hydrogen atoms were refined with anisotropic thermal parameters.

(11) Sheldrick, G. M. *Acta. Crystallogr*. **1990**, *A46*, 467−473.
(12) Sheldrick, G. M. SHELX 76, Program for Crystal Structure Determination, University of Cambridge, 1976.
(13) Walker, N.; Stuart, D, *Acta Crystallogr*. **1983**, *A39*, 158−166.
(14) Johnson, C. K. ORTEP II; Report ORNL-5138; Oak Ridge National Laboratory: Oak Ridge, TN, 1976 (implemented at Manchester Computing Centre).
(15) *International Tables for X-Ray Crystallography*; Kynoch Press: Birmingham, England, 1974; Vol. 4.

Results and Discussion

Synthetic Studies. The *para*, *meta*, and *ortho* amino-substituted tetraphenylporphyrins [5-(NH$_2$C$_6$H$_4$)-10,15,20-Ph$_3$porphH$_2$] were obtained from the corresponding nitro derivatives,[8] the latter being formed by reaction of the appropriate nitrobenzaldehyde with pyrrole. The yields of the nitro products were variable (5−24%) and generally in the order *para* > *ortho* > *meta*. Their reduction by $SnCl_2$/HCl afforded virtually quantitative yields of the anilinoporphyrins.[9]

Treatment of [5-(NH$_2$C$_6$H$_4$)-10,15,20-Ph$_3$porphH$_2$] with [Mo(NO)Tp*Cl$_2$] in the presence of NEt$_3$ afforded the desired amido complexes **1**−**3**. Again, the yields were variable and in the order *para* > *ortho* > *meta*. Satisfactory elemental analyses were obtained for these new compounds, although the data obtained from the *ortho* isomer indicated the presence of hexane in the sample, as also found by ^{1}H NMR spectroscopy and in the structural study. High-resolution accurate mass measurements (HRLSIMS) were also made on **2** and **3**, and the molecular structure of the *ortho* complex was confirmed by X-ray crystallography.

IR Spectroscopic Studies. The IR spectra of the new complexes exhibited absorptions characteristic of Tp* (ν_{BH} 2530−2545 cm^{-1}; ν_{C-Me} 1360−1438 cm^{-1}) and the porphyrin (ν_{CH} 2840−2920 cm^{-1}; $\nu_{C=C}$ 1532−1535 cm^{-1}; ν_{NH} 3310, 3245−3285 cm^{-1}). The NO stretching frequencies of the [Mo(NO)Tp*Cl] moiety, in the range 1652−1660 cm^{-1}, were consistent with the values expected for amido complexes,[6] being 8−22 cm^{-1} lower than those in the corresponding phenolato species [5-{[Mo(NO)Tp*Cl]OC$_6$H$_4$}-10,15,20-Ph$_3$porphH$_2$]. This reflects the stronger electron-donating properties of the amido group compared to the phenolato ligand. The slightly lower value of ν_{NO} in **3** might appear to suggest that the amido group in this species is a marginally better donor than those in the other two isomers, although the shift in frequency is very small. By analogy with [5-{*o*-([Mo(NO)Tp*Cl]O)C$_6$H$_4$}-10,15,20-Ph$_3$porphH$_2$], the shift could be associated with approach of the [Mo(NO)Tp*Cl] moiety to the macrocyclic ring (see below).

Electronic Absorption Spectra. The electronic spectral data for the new complexes and their precursor ligands, in dichloromethane and dimethylformamide, are summarized in Table 5. The metalated and unmetalated porphyrins have similar and characteristic spectra, being little perturbed by the peripheral substituents. However the $Q_y(0,0)$ band in the spectrum of **1** is bathochromically shifted in both dichloromethane and DMF, by 7 and 5 nm, respectively, with respect to its unmetalated precursor. These are only small increments, being equivalent at most to *ca.* 3 kJ mol^{-1} or *ca.* 28 mV. The absorption bands of **3** in dichloromethane are bathochromically shifted by up to 4 nm with respect to [5-(*o*-NH$_2$C$_6$H$_4$)-10,15,20-Ph$_3$porphH$_2$].

^{1}H NMR Spectra. The labeling scheme for the ^{1}H NMR spectral data obtained from the new compounds is shown in Figure 1. The signals associated with the porphyrin moiety and the Tp* ligand generally occur in the expected regions. The NH proton of the amido group generally appears in the range $\delta = 12.87-12.96$ ppm, at such a high frequency partly because of the electron-withdrawing nature of the [Mo(NO)Tp*Cl] group. The protons attached to C-4 of the pyrazolyl rings in Tp* ($\delta = 5.81-5.96$ ppm) generally occur as three singlets of relative area 1:1:1 because of the asymmetry of the {[Mo(NO)Tp*Cl]NHAr} moiety (there is no plane of symmetry containing the H−B···Mo axis). The methyl signals of the pyrazolyl rings also generally occur as singlets ($\delta = 2.34-2.77$ ppm), and only in the case of the *meta* isomer is there some overlap.

Table 2. Fractional Atomic Coordinates ($\times 10^4$) with esd's in Parentheses

	x	*y*	*z*		*x*	*y*	*z*
Mo(1)	6339(1)	1910(1)	2254(1)	C(24)	824(16)	3293(12)	−556(10)
Cl(1)	7248(4)	3131(4)	2256(2)	C(25)	568(19)	3137(16)	−1082(10)
N(1)	4063(10)	1019(10)	597(6)	C(26)	−263(21)	3443(18)	−1283(14)
N(2)	5232(10)	2206(10)	83(6)	C(27)	−847(25)	3885(26)	−1014(16)
N(3)	3507(10)	2967(10)	−293(6)	C(28)	−691(20)	4014(17)	−536(17)
N(4)	2331(11)	1770(10)	208(6)	C(29)	173(18)	3716(19)	−291(12)
N(5)	5306(11)	960(9)	2376(7)	C(30)	1617(15)	2221(14)	−22(8)
N(6)	4352(12)	1094(11)	2508(7)	C(31)	675(14)	1907(16)	120(9)
N(7)	5129(14)	2587(10)	1876(6)	C(32)	832(13)	1274(16)	438(9)
N(8)	4182(12)	2367(11)	2002(8)	C(33)	1916(15)	1186(13)	464(9)
N(9)	5648(11)	2320(10)	2945(7)	C(34)	2388(13)	594(13)	745(8)
N(10)	4615(12)	2438(9)	2920(7)	C(35)	1805(13)	−34(13)	1031(8)
N(11)	7305(10)	1397(9)	2557(6)	C(36)	1338(22)	−628(18)	750(11)
N(12)	6557(10)	1537(10)	1579(6)	C(37)	797(20)	−1176(20)	982(12)
O(1)	7996(11)	1114(10)	2770(6)	C(38)	718(17)	−1196(15)	1454(15)
C(1)	7105(13)	992(13)	1320(8)	C(39)	1178(20)	−593(19)	1759(11)
C(2)	8015(15)	640(14)	1497(10)	C(40)	1719(20)	−7(18)	1523(9)
C(3)	8479(14)	113(15)	1211(10)	C(41)	3372(16)	513(11)	795(8)
C(4)	8113(16)	−193(16)	771(9)	C(42)	3893(19)	−65(15)	1087(10)
C(5)	7324(16)	169(16)	554(10)	C(43)	4891(16)	73(14)	1034(10)
C(6)	6820(14)	707(15)	834(9)	C(44)	4969(12)	737(12)	719(8)
C(7)	5844(14)	1031(15)	578(9)	C(45)	6332(17)	−293(13)	2291(9)
C(8)	5976(13)	1741(13)	280(7)	C(46)	5396(15)	160(16)	2405(8)
C(9)	6903(13)	2090(16)	159(9)	C(47)	4551(21)	−214(16)	2545(10)
C(10)	6720(13)	2747(15)	−118(7)	C(48)	3921(16)	429(16)	2620(8)
C(11)	5679(13)	2797(13)	−163(8)	C(49)	2848(16)	459(15)	2811(10)
C(12)	5221(14)	3458(14)	−404(7)	C(50)	5875(15)	3372(13)	1191(8)
C(13)	5829(15)	4123(14)	−623(9)	C(51)	5035(15)	2936(11)	1434(9)
C(14)	6364(16)	4606(15)	−299(9)	C(52)	4055(16)	2923(15)	1264(10)
C(15)	6983(16)	5174(17)	−488(13)	C(53)	3542(15)	2619(13)	1641(10)
C(16)	7066(16)	5266(16)	−1013(10)	C(54)	2493(19)	2501(19)	1650(12)
C(17)	6524(18)	4783(16)	−1328(10)	C(55)	6987(14)	2689(16)	3534(8)
C(18)	5912(17)	4222(14)	−1139(9)	C(56)	6010(17)	2688(14)	3349(10)
C(19)	4160(16)	3498(14)	−492(8)	C(57)	5148(19)	2966(13)	3645(11)
C(20)	3655(16)	4116(13)	−777(9)	C(58)	4321(15)	2769(15)	3353(8)
C(21)	2670(14)	3922(14)	−735(8)	C(59)	3286(15)	2948(14)	3475(10)
C(22)	2601(13)	3242(13)	−444(7)	B(1)	4038(21)	1985(22)	2515(12)
C(23)	1721(12)	2867(15)	−336(7)				

Table 3. Distance (Å) of Atoms from the N(1)−C(44)−C(7)−C(8)−N(2)−C(11)−C(12)−C(19)−N(3)−C(22)−C(23)−C(30)−N(4)−C(33)−C(34)−C(41) Plane

atom	3	atom	3
N(1)	+0.04	N(3)	−0.01
C(44)	−0.01	C(22)	−0.02
C(7)	−0.08	C(23)	−0.10
C(8)	−0.06	C(30)	−0.03
N(2)	−0.01	N(4)	+0.01
C(11)	0.00	C(33)	+0.03
C(12)	+0.12	C(34)	+0.05
C(19)	+0.03	C(41)	+0.03

[a] Esd's are *ca.* 0.03 Å.

Table 4. Selected Bond Lengths (Å) and Bond Angles (deg) for **3**[a]

Distances			
Mo−N(5)	2.151(16)	Mo−Cl	2.383(7)
Mo−N(7)	2.220(18)	Mo−N(H)	1.928(16)
Mo−N(9)	2.194(17)	N(H)−C(1)	1.374(26)
Mo−N(O)	1.752(14)	Mo...B	3.244
N(O)−O	1.184(21)		

Angles			
N(5)−Mo−N(7)	87.5(6)	N(9)−Mo−N(O)	96.0(6)
N(5)−Mo−N(9)	78.7(6)	N(9)−Mo−Cl	88.2(4)
N(5)−Mo−N(O)	93.6(7)	N(9)−Mo−N(H)	163.3(6)
N(5)−Mo−Cl	166.4(5)	Cl−Mo−N(O)	91.6(5)
N(5)−Mo−N(H)	91.2(7)	Cl−Mo−N(H)	100.6(5)
N(7)−Mo−N(9)	83.5(6)	N(H)−Mo−N(O)	97.8(7)
N(7)−Mo−N(O)	178.7(7)	Mo−N(H)−C(1)	141.2(14)
N(7)−Mo−Cl	87.1(5)	Mo−N−O	174.2(15)
N(7)−Mo−N(H)	82.8(6)		

Torsion Angle (deg)	
N(O)−Mo−NH−C(1)	+9.0

[a] Esd's are in parentheses.

The central NH protons of the porphyrin ring resonate in the region from −2.73 to −2.92 ppm, their shift in **3** being somewhat higher than for **1** and **2** (by *ca.* 0.2 ppm).

The signals due to the pyrrolyl protons generally occur in the region $\delta = 8.84-8.93$ ppm, those due to the protons of rings A and B appearing as an A_2B_2 multiplet. In the *para* and *meta* isomers, these signals occur at a higher frequency than those of rings C and D, presumably because of the electron-withdrawing influence of the [Mo(NO)Tp*Cl] group. In these isomers, the protons of rings C and D appear as a singlet.

In all three isomers, the *ortho* protons of the unsubstituted porphyrin phenyl rings afford an unresolved multiplet in the range $\delta = 8.05-8.27$ ppm, whereas the *meta* and *para* protons generate an unresolved multiplet at $\delta = 7.75-7.78$ ppm. These differences in shifts can be explained by the effects of the porphyrin ring current. The substituted phenyl ring protons generally resonate at $\delta = 7.88-8.33$ ppm. In the *para* isomer, they occur as two doublets ($J = 8.4$ Hz), the signals at higher frequency being assigned to H_p and $H_{p'}$. In the *meta* isomer, the spectrum, from high to low frequency, appears as two doublets, a singlet, and a doublet of doublets (appearing as a triplet). These signals are assigned to H_q/H_s, H_q/H_s, H_p and H_r, respectively. The doublets and doublets of doublets have $J \approx 8$ Hz. In the spectrum of **3**, the substituted phenyl ring protons appear as an overlapping doublet, an overlapping doublet of doublets (appearing as a triplet), and a further doublet of doublets (also appearing as a triplet), with one proton signal appearing unusually shifted to higher frequency and being

Table 5. Electronic Spectra of [5-(RC_6H_4)-10,15,20-$Ph_3PorphH_2$] (R = NO_2, NH_2, or NHMo(NO)Tp*Cl)

compound/R	solvent	B λ^a (ϵ)^b	$Q_y(1,0)$ λ^a (ϵ)^c	$Q_y(0,0)$ λ^a(ϵ)^d	$Q_x(1,0)$ λ^a (ϵ)^d	$Q_x(0,0)$ λ^a(ϵ)^d
R = *p*-NO_2	CH_2Cl_2	417 (3.7)	514 (1.9)	549 (8.7)	588 (5.7)	644 (4.3)
	DMF	416 (4.2)	512 (1.9)	547 (8.9)	588 (5.8)	644 (4.7)
R = *m*-NO_2	CH_2Cl_2	417 (4.0)	513 (1.8)	548 (7.2)	588 (5.4)	645 (4.0)
	DMF	416 (2.5)	512 (1.1)	547 (4.7)	588 (3.3)	644 (2.4)
R = *o*-NO_2	CH_2Cl_2	417 (4.0)	513 (1.7)	548 (6.6)	589 (5.2)	645 (3.2)
	DMF	417 (3.0)	513 (1.2)	547 (4.6)	589 (3.3)	645 (2.6)
R = *p*-NH_2	CH_2Cl_2	419 (2.8)	514 (1.6)	551 (8.1)	589 (5.2)	646 (3.8)
	DMF	416 (3.0)	514 (1.5)	550 (7.6)	589 (4.8)	647 (4.2)
R = *m*-NH_2	CH_2Cl_2	417 (2.8)	513 (1.2)	548 (4.6)	589 (3.4)	644 (2.7)
	DMF	417 (3.7)	513 (1.8)	548 (7.3)	589 (5.2)	645 (4.2)
R = *o*-NH_2	CH_2Cl_2	416 (3.5)	513 (1.7)	547 (6.3)	588 (5.0)	644 (3.7)
	DMF	415 (4.3)	513 (2.0)	548 (8.0)	589 (5.9)	646 (4.6)
1	CH_2Cl_2	416 (2.6)	515 (2.7)	558 (1.5)^c	588 (1.2)^c	649 (7.7)
	DMF	416 (2.6)	512 (2.7)	555 (1.6)^c	587 (1.1)^c	648 (7.8)
2	CH_2Cl_2	416 (2.9)	514 (2.4)	549 (1.0)^c	589 (6.9)	645 (4.5)
	DMF	416 (2.2)	513 (1.5)	548 (7.7)	588 (5.2)	643 (3.8)
3	CH_2Cl_2	417 (2.5)	515 (2.0)	551 (8.9)	590 (6.4)	647 (4.0)
	DMF	417 (2.6)	514 (1.8)	549 (7.8)	589 (5.4)	646 (3.7)

^{a} In nm. ^{b} ϵ in mol^{-1} L·cm^{-1} × 10^5. ^{c} ϵ in mol^{-1} L·cm^{-1} × 10^4. ^{d} ϵ in mol^{-1} L.cm^{-1} × 10^3, as calculated by the Beer−Lambert law.

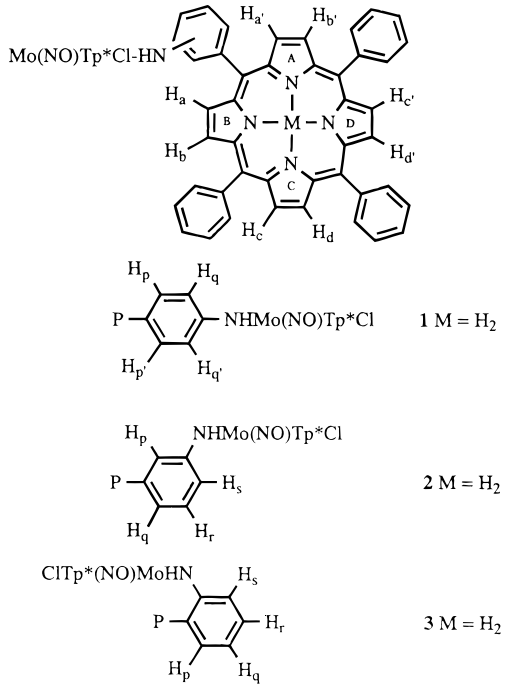

Figure 1. Atom labeling in extraring molybdenated porphyrin complexes.

obscured by the multiplet due to the pyrrole protons of rings C and D. These signals could not be unambiguously assigned.

A notable exception to these generalizations concerns the ^{1}H NMR spectrum of **3**. It was noted that the pyrrolyl protons, from high to low frequency, gave rise to a singlet, an unresolved multiplet, and two AB systems. The singlet and multiplet were assigned to the pyrrolyl protons of rings C and D, although we did not establish which pair of protons gave rise to each set of signals. The AB multiplets appear to lower frequency of the equivalent resonances due to H_a, $H_{a'}$, H_b, and $H_{b'}$ in the *para* and *meta* isomers of [5-{[Mo(NO)Tp*Cl]NHC_6H_4}-10,15,20-$Ph_3PorphH_2$], presumably because of the relatively close proximity of the [Mo(NO)Tp*Cl] moiety to the macrocyclic ring, as has been observed in [5-{*o*-([Mo(NO)Tp*Cl]O)C_6H_4}-10,15,20-$Ph_3PorphH_2$].[4] The AB multiplets could not be unambiguously assigned. Other unusual features are the shifts to lower frequency, by *ca.* 0.2 and *ca. 0.6* ppm, respectively, of the central NH protons of the porphyrin and the NH proton of the amido group. Further, while all of the pyrazolyl ring protons of Tp* appear at δ values to lower frequency of those in **1** and **2**, one pyrazolyl ring proton exhibits a much larger shift to lower frequency than the other Tp* protons, appearing at δ = 2.82 ppm rather than at *ca.* 5.9 ppm.

Table 6. Proton Labeling Used in NOE Investigations of **3**

label	δ (ppm)	assignment
CH^1	5.62	pyrazolyl ring
CH^2	5.60	protons
CH^3	2.82	Me_2C_3HN
Me^1	2.52	
Me^2	2.46	pyrazolyl methyl
Me^3	1.96	protons
Me^4	1.85	$(CH_3)_2C_3HN_2$
Me^5	0.93	
Me^6	0.52	

These observations suggest that there may be a close approach of at least one of the pyrazolyl rings in Tp* to part of the porphyrin ring because of the steric arrangements of the *ortho*-substituted {[Mo(NO)Tp*Cl]NHC_6H_4} moiety, as has been observed in [5-{*o*-([Mo(NO)Tp*Cl]O)C_6H_4}-10,15,20-Ph_3-$porphH_2$].[4] However, these effects are not so dramatic as in [5-{*o*-([Mo(NO)Tp*Cl]O)C_6H_4}-10,15,20-$Ph_3PorphH_2$], suggesting that the interactions may not be so close. Examination of the molecular structure of **3** reveals that, in contrast to the structural arrangements in [5-{*o*-([Mo(NO)Tp*Cl]O)C_6H_4}-10,15,20-$Ph_3PorphH_2$],[4] there is not such a close approach of the pyrazolyl rings in Tp* to the porphyrin ring in **3**, all interactions being greater than 3 Å. To further investigate the possibility of a close interaction between at least one of the pyrazolyl rings in Tp* and part of the porphyrin ring in solution, a 2D-NOESY experiment was performed. The protons in the pyrazolyl rings are assigned as follows (the labeling of the H and methyl protons is shown in Table 6): ring 1, Me^2, Me^4, CH^1; ring 2, Me^1, Me^3, CH^2; ring 3, Me^5, Me^6, CH^3. Additionally, NOEs were found between Me^2 and the multiplet at 8.82 ppm (H_p/H_s of $NHC_6H_4PorphH_2$ and pyrrole protons of rings C and D), and the multiplet at 8.49 ppm (H_a,H_b or $H_{a'}$,$H_{b'}$, pyrrole protons of rings A and B). Furthermore, an NOE was found between Me^6 and the AB multiplet at 8.72 ppm (H_a,H_b or $H_{a'}$,$H_{b'}$, pyrrole protons of rings A and B). These results suggest that the faces of rings A, B, and possibly C in the porphyrin are in close proximity to the pyrazole rings 1 and 3 in Tp*.

Electrochemical Studies. The electrochemical properties of the new complexes were investigated by cyclic voltammetry (Table 7, Scheme 1). Plots of i_{pa} *vs* (scan rate)$^{1/2}$ gave slight deviations from linearity (a slight downward curvature), which may be due to slow electron transfer. Multiple scans for each

Table 7. Electrochemical Data Obtained from **1**−**3**

	porphyrin				
	oxidation		reduction		
compound	$E_f(1)^b$ (ΔE_p)^c	$E_f(2)^b$ (ΔE_p)^c	$E_f(3)^b$ (ΔE_p)^c	$E_f(4)^b$ (ΔE_p)^c	Mo reduction^a $E_f(5)^b$ (ΔE_p)^c
[$Ph_4porphH_2$]	+1.11^d	+1.36^d	−1.08^d	−1.43^d	
1	+1.07 (110)^d	+1.35 (165)^d	−1.17 (85)^d	−1.56 (150)^d	−0.75 (100)^d
2	+1.12 (100)^d	+1.38 (110)^d	−1.13 (95)^d		−0.78 (115)^d
3	+1.18 (70)^d	+1.40 (100)^d	−1.17 (75)^d	−1.57 (95)^d	−0.77 (80)^d

^{a} Reduction of {Mo(NO)Tp*X}, in dry CH_2Cl_2 *vs* SCE using Pt bead working electrode; scan rate, 200 mV s^{-1}; 0.2 M [*n*-Bu_4N][BF_4]. ^{b} In volts (±0.01 V). ^{c} In millivolts (±10 mV). ^{d} Ferrocene was used as an internal standard and under the same conditions gave E_f for the couple $[Fe(C_5H_5)_2]/[Fe(C_5H_5)_2]^+ = +0.54 \pm 0.01$ V ($\Delta E_p = 80$ mV).

Scheme 1. Redox Products of Complexes **1**-**3**

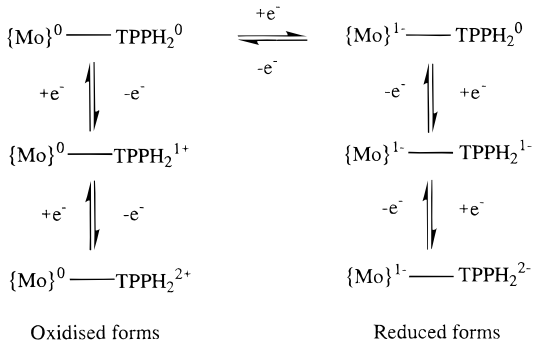

{Mo} = {Mo(NO)Tp*Cl(NHC$_6$H$_4$-)}

$TPPH_2$ = triphenylporphyrin

compound showed that the cathodic and anodic currents were not constant but decayed with time. Since each of the reduction and oxidation processes had $i_{pa}/i_{pc} = 1.0 \pm 0.1$, this decay in peak current may be due to electrode coating. The values of ΔE_p for the complexes are in the range 70−165 mV. Under similar conditions, the ferrocene/ferrocenium couple gave ΔE_p values of 70−80 ± 10 mV, compared to the theoretical ΔE_p value of 59 mV for a reversible one-electron transfer. Thus, some 10−20 mV of the ΔE_p values may arise from junction potentials and/or uncompensated resistances in the electrochemical cell. The general electrochemical behavior of the compounds indicates that their electrode behavior ranges from reversible through quasi-reversible to irreversible processes.

The *para* and *ortho* complexes exhibit five redox processes (Scheme 1). The *meta* isomer **2** exhibits broadly similar behavior, but the second porphyrin-based reduction process (third reduction process of the complete compound) was obscured by the solvent decomposition. The first (least negative) reduction process is associated with the [Mo(NO)Tp*Cl] fragment. The values of E_f for this reduction lie in the range from −0.75 to −0.78 ± 10 mV *vs* SCE and are very similar to the reduction potentials in related amido species ([Mo(NO)-Tp*Cl]NHAr).[16] The small potential differences between the isomers are not significant. The E_f values of these amide complexes are more anodic than those of their phenoxy analogues, [5-{[Mo(NO)Tp*Cl]OC_6H_4}-10,15,20-$Ph_3porphH_2$][4] (*ca.* 0.44 V), because of the more effective π-donor capacity of the anilido fragment when compared with that of the phenoxide.

The remaining reduction processes are associated with the porphyrin ring. Because the molybdenum-containing moiety is reduced before the porphyrin ring, the electroactive species is already anionic before charge transfer to the porphyrin ring occurs. Thus, the E_f values for the latter are between 50 and 90 mV more cathodic for the first reduction and *ca.* 140 mV more cathodic for the second porphyrin reduction than the corresponding processes in unmetalated [$Ph_4porphH_2$]. The two oxidation processes observed for these compounds are associated with the porphyrin ring. In the cases of **1** and **2**, their potentials are virtually unaltered upon metalation. However, the first oxidation potential of **3** is 70 mV more positive than the comparable process in [$Ph_4porphH_2$].

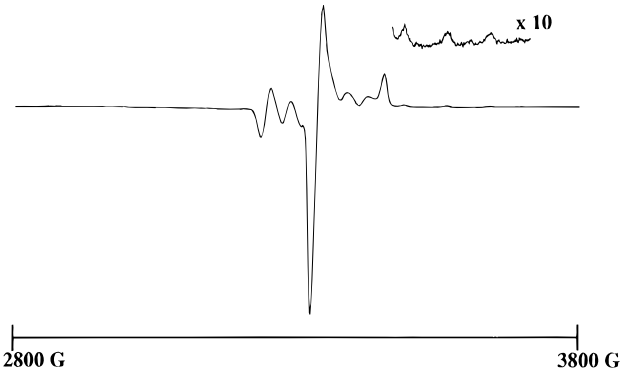

Figure 2. EPR spectrum of the electrochemically reduced 17-electron form of **1** at 77 K.

EPR Spectral Studies. The site of the first electron reduction process of the molybdenum moiety was confirmed using EPR spectroscopy. The starting complex containing the 16-electron molybdenum center may be electrochemically reduced to give the 17-electron form, **1**$^-$, which has a characteristic signal at room temperature with $g_{iso} = 1.979 \pm 0.001$, and a hyperfine coupling constant of 4.53 ± 0.05 mT for an unpaired electron strongly coupled to a molybdenum center.[17] At 77 K, the 17-electron form of **1** gives an axial spectrum (Figure 2) with $g_{(parallel)} = 1.932 \pm 0.001$ and $g_{(perpendicular)} = 2.004 \pm 0.001$, and with $A_{(parallel)} = 7.47 \pm 0.05$ mT and $A_{(perpendicular)} = 3.49 \pm 0.05$ mT. $(2A_{(perpendicular)} + A_{(parallel)})/3 \approx A_{iso}$, and therefore $A_{(perpendicular)}$, $A_{(parallel)}$, and A_{iso} all have the *same* sign. $g_{iso} \approx g_{av} = (2g_{(perpendicular)} + g_{(parallel)})/3$.) Coupling with other nuclei was not observed under the conditions of the experiment. These findings are typical for the 17-electron form of the [Mo(NO)-Tp*Cl] group[4] and demonstrate that the molybdenum is the site of the first reduction process, and hence the most likely receptor for the transferred electron in the photoinduced electron transfer process.

(16) Al Obaidi, N.; Clague, D.; Chaudhury, M.; Jones, C. J.; McCleverty, J. A.; Pearson, J. C.; Salam, S. S. *J. Chem. Soc., Dalton Trans.* **1987**, 1733−1736.

(17) Molybdenum has two spin-active isotopes with spin $^5/_2$; hence, it was expected to observe a six-line signal due to these isotopes, with a large unsplit central signal due to the remaining molybdenum isotopes with no nuclear spin. The two molybdenum spin-active isotopes, $^{95}_{42}$Mo and $^{97}_{42}$Mo (natural abundances 15.72% and 9.46%), have very similar nuclear magnetic moments of −0.913 and −0.933 μ_N. The hyperfine coupling constants are, therefore, sufficiently similar that two sets of signals cannot be distinguished, and the spectra can be adequately explained by considering that 25.2% of the signal intensity is split into a 1:1:1:1:1:1 sextet, with the other 74.8% as a central single peak.

Table 8. Redox Potentials and Transient Lifetimes

compound	E_f(Mo)/ V[a]	E_f(porph)/ V[a]	τ_{CS}/ps	τ_{CR}/ps	$\Delta G°$/eV CS[e]	$\Delta G°$/eV CR[e]
1	−0.75	1.07	4[b]	300[c] (98%)[d]	−0.06	−1.82
2	−0.78	1.12	12[b]	325[c] (44%)[d]	0.02	−1.90
3	−0.77	1.18	8[b]	340[c] (8%)[d]	0.07	−1.95

[a] *Vs* standard calomel electrode (SCE), measured in dichloromethane containing 0.2 mol dm^{-3} [*n*-Bu_4N][BF_4] at a Pt bead electrode. Fc/$Fc^+ = +0.54 \pm 0.01$ V; E_f(Mo) is the first reduction potential associated with the [Mo(NO)Tp*] moiety, and E_f(porph) is the first oxidation potential associated with the porphyrin moiety. [b] Lifetime for charge separation ± 10%, measured in DMF at *ca.* 680 nm. [c] Lifetime for charge recombination ± 10%, measured in DMF at *ca.* 680 nm. [d] Percentage of component with long τ. This probably reflects the slight differences between the excited state UV spectra of **1**−**3** at 680 nm. [e] CS, charge separation; CR, charge recombination. Calculated as $\Delta G°(CS) = E_f^1 - E_f^2 - E_{singlet} + w^*$ and $\Delta G°(CR) = E_f^2 - E_f^1 - w^*$, where E_f^1 and E_f^2 are the measured half-wave potentials for oxidation of the porphyrin and reduction of the [Mo(NO)Tp*] moiety, respectively, $E_{singlet}$ is the energy of the first excited singlet state of the porphyrin, and w^* is the Coulombic work term, which here was ignored as it is negligible in DMF.

Photochemical Studies. Preliminary picosecond spectroscopic studies of **1** in dimethylformamide provided evidence for the fast ($k > 33 \times 10^9$ s^{-1}; $\tau < 30$ ps) formation of the porphyrin radical cation, which decayed following first-order kinetics with a rate of $(3.5 \pm 1.2) \times 10^9$ s^{-1}, corresponding to a lifetime of 290 ± 110 ps.[5] Using a value of 1.88 eV for $E_{singlet}$ (as for [$Ph_4porphH_2$]), and neglecting solvent effects, the $\Delta G°$ values for charge separation in **1**−**3** are calculated to be −0.06, 0.02, and 0.07 eV, respectively (Table 8). In view of the apparent observation of charge separation in **1**, despite a near zero driving force, further photochemical studies were carried out to confirm the findings for **1** and to determine whether **2** and **3** show similar behavior.

All three complexes exhibit luminescence quenching, and femtosecond transient absorption measurements were made on *ca.* 10^{-4} M solutions of **1**−**3** in dimethylformamide (DMF) (Table 8). Typically, the spectra show broad absorptions at *ca.* 620 and 680 nm and broad bleaching bands at *ca.* 600 and 660 nm. The characteristic broad absorption at *ca.* 680 nm in the spectra of **1**−**3** again provided evidence for the fast ($\tau = 4-12$ ps) formation of the porphyrin radical cation, which decayed following first-order kinetics with lifetimes of 300−340 ps. In the less polar solvent toluene, the charge separation rate measured at 650 nm for **1** is slower ($\tau = 17$ ps), but the charge recombination rate is faster ($\tau = 186$ ps). Spectroelectrochemical UV/vis studies have shown that the reduced 17-electron complex [Mo(NO)Tp*Cl(OPh)]$^-$ absorbs below 400 nm, but unfortunately it was not possible to observe its formation and decay, as it was only possible to monitor the transient spectra between 400 and 800 nm. However, the rates of the charge separation and charge recombination are consistent with *intra*molecular processes, and electrochemical techniques show that the molybdenum nitrosyl center has the lowest reduction potential. In addition, spectroelectrochemical EPR studies showed that the one-electron reduction of complex **1** affords a complex containing the 17-electron molybdenum center, so it may be assumed that the molybdenum atom acts as the acceptor in these complexes.

The formation of the porphyrin radical cation is fast enough to compete effectively with intersystem crossing to the triplet state, which would otherwise be observed in the transient decay spectra after 1 ns. [The $\Delta G°$ values for charge separation between the triplet state and the molybdenum nitrosyl center in **1**−**3**, based on the value of 1.43 eV for $E_{triplet}$ in [$Ph_4porphH_2$], are respectively +0.39, +0.47 and +0.52 eV. If formed, the triplet state would not be expected to quench *via* charge separation involving the molybdenum and so should persist into the nanosecond time domain.]

The rates of charge recombination for **1**−**3** are slower than those found for the analogous compounds containing {Mo−OC_6H_4−porphyrin} links in place of {Mo−NHC_6H_4−porphyrin}. This is consistent with the rates of charge recombination being in the Marcus inverted region, so that the more exergonic $\Delta G°$ values for charge recombination (−1.82 to −1.95 eV for {Mo−NHC_6H_4−porphyrin} compared to −1.38 to −1.43 eV for {Mo−OC_6H_4−porphyrin}) lead to lower rates. More puzzling is the observation that fast charge separation occurs in systems that have near zero driving force for the process. This implies a small reorganization energy for the acceptor site. No data on this are available for the {[Mo(NO)Tp*Cl]NH-C_6H_4-} moiety but the vibrational reorganization energy of {Ru-$(NH_3)_5$}$^{2+}$ has been estimated[18] at 0.1 eV, which may be compared to values in the region 0.5−1.2 eV for quinone acceptors.[19] This suggests that lower reorganization energies may, indeed, be involved in the case of electron transfers to d-block metal centers. The variation in charge separation rates with metal porphyrin separation is another point of interest in these systems. However, Hupp has proposed that, in the case of mixed-valence charge transfer in [{$Ru(NH_3)_5$}$_2$(4,4′-bpy)]$^{5+}$, the electron acceptor should be thought of as the {$Ru(NH_3)_5$-NC_5H_4-}$^{3+}$ moiety, not {$Ru(NH_3)_5$}$^{3+}$. If similar arguments can be applied in the cases of **1**−**3**, the acceptor group in each case would be {Mo(NO)Tp*NHC_6H_4-}, so that the porphyrin acceptor distance is now invariant. This would be in accord with the insensitivity of the charge recombination rates to metal−porphyrin distance, over the range 6−10 Å, as found for **1**−**3**. If such distance effects are, indeed, unimportant in these compounds, the charge separation rate may be dominated by electronic coupling between the metal and the porphyrin centers. The lowest charge separation rate is found for **2** with a *meta*-substituted aryl link in which mesomeric contact between the {Mo−NH} and porphyrin substituents is absent. The lower rate for **3** compared to that for **1** may be the result of steric effects. The orientation of the thioaryl groups in [Mo(η^5-C_5H_5)-(NO)$(SPh)_2$] and related compounds has been found to affect the extent of overlap between the unoccupied Mo d_{xy} orbital and filled p-orbitals on sulfur.[20] Thus, in **3**, the possibility exists that steric interactions that alter the torsion angle about the Mo−NH bond may lead to a less than optimum structural arrangement for electronic coupling, giving rise to a slower charge separation rate than for the *para*-substituted system.

Structural Studies. The compound **3** crystallizes from CH_2Cl_2/*n*-hexane as poorly-formed dark purple plates. While refining the crystal structure, we found that the unit cell contained an additional molecule partially occupying a lattice site. This was probably an associated solvent molecule, possibly hexane, but all attempts to determine its identity from the X-ray data failed. The high *R* values (see Experimental Section) may be attributed to this. Stoichiometric and nonstoichiometric solvent inclusion by crystals of compounds containing the [Mo(NO)Tp*] moiety is quite common,[21−26] and crystals may decrepitate if this solvent is removed by excessive drying. The

(18) Hupp, J. T.; Dong, Y.; Blackbourn, R. L.; Lu, H. *J. Phys. Chem.* **1993**, *97*, 3278−3282.
(19) Schmidt, J. A.; Liu, J.-Y.; Bolton, J. R.; Archer, M. D.; Gadzekpo, V. P. Y. *J. Chem. Soc., Faraday Trans.* **1989**, *85*, 1027−1041.
(20) Ashby, M. T.; Enemark, J. A. *J. Am. Chem. Soc.* **1986**, *108*, 730. Al Obaidi, N.; Jones, C. J.; McCleverty, J. A. *Polyhedron* **1989**, *8*, 1033−1037.

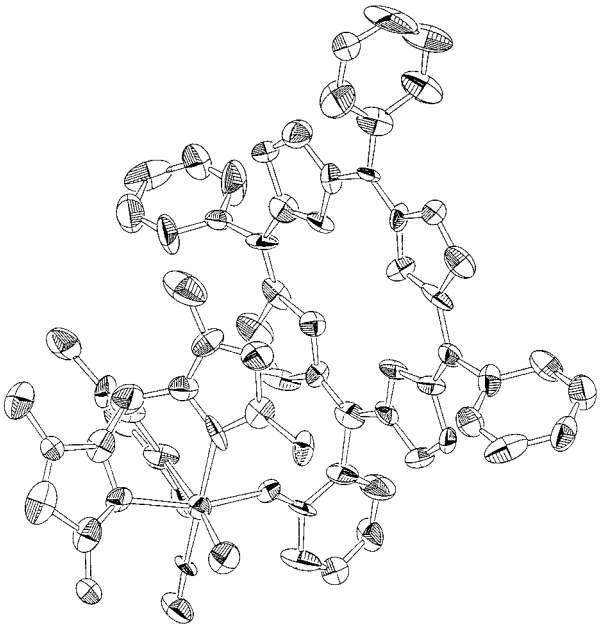

Figure 3. Molecular structure of **3**.

structure is shown in Figure 3, results of mean-plane calculations are in Table 3, and selected bond distances and angles are in Table 4.

Tetraphenylporphyrin itself occurs in two crystalline forms. Because of crystallographic symmetry in the tetragonal form,[27] the imino hydrogen atoms are equally distributed, with a statistical population of only half a hydrogen atom on each nitrogen atom. In the triclinic form,[28] the hydrogen atoms are localized on one pair of nitrogen atoms. The porphyrin central NH hydrogen atoms of **3** could not be found on the difference Fourier map and so were not included.

The bond lengths and bond angles obtained for the porphyrin moiety in **3** (Table 3) are in agreement with those obtained for tetraphenylporphyrin, within the rather large experimental error.[27,28] The porphyrin skeleton in the tetragonal form of [Ph_4-porphH_2][27] is ruffled, *i.e.*, there is a deformation of the porphyrin skeleton below the plane of the macrocycle ring, as defined by the inner ring atoms, in the first and third quadrants and above the plane of the porphyrin ring in the second and fourth. Maximum deviations, alternately above and below the ring plane, occur at the methine carbon atoms with the nitrogen atoms close to the plane. Calculations of the deviations of the atoms from the mean-plane of the porphyrin ring in **3** also show that the porphyrin inner ring is not planar, but ruffled, with atomic deviations of up to 0.12 Å (Table 2), with maximum deviations occurring at the methine carbon atoms, C(7), C(12), C(23), and C(34). Although the ruffling does not conform to the precise $\bar{4}$ (S_4) symmetry of tetragonal tetraphenylporphyrin, and atomic deviations are smaller, the overall shapes of the rings are similar.

The porphyrin phenyl rings in **3** (structure shown in Figure 3) are planar to within experimental error and are twisted relative to the porphyrin plane. The four phenyl rings in the compound are at angles of 92, 114, 105, and 106° (±2°) relative to the macrocycle plane. The phenyl ring rotation is expected, since otherwise the phenyl hydrogen atoms proximal to the porphyrin ring would interfere with the pyrrole hydrogen atoms.[29]

The angles at molybdenum reported in Table 3 indicate that the molybdenum atom has a slightly distorted octahedral coordination. Of the *trans* angles, the minimum angular deviation from the ideal octahedral angle of 180° occurs for the N−Mo−N(O) angle, whereas the other two angles deviate by larger amounts from ideality. This is in accord with the structures of other {Mo(NO)Tp*X} moieties.[6a,21−26]

The pyrazolyl rings are virtually planar, and the methyl groups lie close to their respective ring planes, whereas the metal and boron atoms deviate by greater amounts, 0.76 and 0.19 Å (±0.05 Å). As expected, the smallest dihedral angle is between the pyrazolyl rings encompassing the relatively small nitrosyl ligand.

As usually found in this class of complexes, the molybdenum−nitrosyl fragment is nearly linear.[30] A study carried out on five amido complexes[22−24] has shown that the mean value for the Mo−N−O angle is 176.7(13)° (minimum 174(3)°, maximum 179.6(10)°). Such a nearly linear Mo−N−O arrangement allows the nitrosyl group to act as a three-electron donor. The mean Mo−N bond length is 1.756(8) Å (minimum 1.70(3) Å, maximum 1.80(2) Å), and the mean N−O bond length is 1.184-(7) Å (minimum 1.16(3) Å, maximum 1.24(4) Å). The values obtained for **3** fall within these ranges. The Mo−N(nitrosyl) bond is the shortest of all the Mo−N bonds (Table 3). The Mo−N bond *trans* to the strongly π-accepting nitrosyl group is the longest of all the Mo−N(pyrazolyl) bonds as a result of the *trans* π-bonding influence, while that *trans* to the halogen is the shortest of all the Mo−N(pyrazolyl) bonds. This is a result of the smaller degree of π-bonding between the molybdenum and the halogen in comparison to that between the molybdenum and the other two monodentate ligands. These findings are consistent with those of previous work.[22−24]

The Mo−Cl bond length is slightly shorter than a pure σ-bond, and consequently, some small degree of π-donation from the halogen to the metal seems probable, as has been discussed previously.[31]

The Mo−NH($TPPH_2$) bond length is relatively short (Table 3), which implies significant pπ-dπ donation from the donor atom (N) to the coordinatively unsaturated metal. The large Mo−N(H)−C(1) angle is also consistent with this view, although steric effects may also play a role in increasing this angle to relieve any close contact between atoms. A study

(21) Denti, G.; Ghedini, M.; McCleverty, J. A.; Adams, H.; Bailey, N. A. *Transition Met. Chem.* **1982**, *7*, 222−224. Wlodarczyk, A.; Edwards, A. J.; McCleverty, J. A. *Polyhedron* **1988**, *7*, 103−115. McCleverty, J. A.; Rae, A. E., Wolochowicz, I.; Bailey, N. A.; Smith, J. M. A. *J. Organomet. Chem.* **1979**, *168*, C1−C7. Adams, H.; Bailey, N. A.; Denti, G.; McCleverty, J. A.; Smith, J. M. A.; Wlodarczyk, A. *J. Chem. Soc., Chem. Commun.* **1981**, 348−350. Obaidi, N. A.; Hamor, T. A.; Jones, C. J.; McCleverty, J. A.; Paxton, K *J. Chem. Soc., Dalton Trans.* **1987**, 2653−2660. Das, A.; Jeffery, J. C.; Maher, J. P.; McCleverty, J. A.; Schatz, E.; Ward, M D.; Wollerman, G. *Angew. Chem., Int. Ed. Engl.* **1992**, *31*, 1515−1518. Das, A.; Jeffery, J. C.; Maher, J. P.; McCleverty, J. A.; Schatz, E.; Ward, M D.; Wollerman, G. *Inorg. Chem.* **1993**, *32*, 2145−2155. Wlodarczyk, A.; Kurek, S. S.; Maher, J. P.; Batsanov, A. S.; Howard, J. A. K.; McCleverty, J. A. *Polyhedron* **1993**, *12*, 715−719.
(22) McCleverty, J. A.; Rae, A. E.; Wolochowicz, I.; Bailey, N. A.; Smith, J. M. A. *J. Chem. Soc., Dalton Trans.* **1982**, 429−438.
(23) McCleverty, J. A.; Denti, G.; Reynolds, S. J.; Drane, A. S.; El Murr, N.; Rae, A. E.; Bailey, N. A.; Adams, H.; Smith, J. M. A. *J. Chem. Soc., Dalton Trans.* **1983**, 81−89.
(24) McCleverty, J. A.; Rae, A. E.; Wolochowicz, I.; Bailey, N. A.; Smith, J. M. A. *J. Chem. Soc., Dalton Trans.* **1983**, 71−80.
(25) Adams, H. A.; Bailey, N. A.; Denti, G.; McCleverty, J. A.; Smith, J. M. A.; Wlodarczyk, A. *J. Chem. Soc., Dalton Trans.* **1983**, 2287−2292.
(26) Al Obaidi, N.; Hamor, T. A.; Jones, C. J.; McCleverty, J. A.; Paxton, K. *J. Chem. Soc., Dalton Trans.* **1987**, 1063−1069.
(27) Hamor, M. J.; Hamor, T. A.; Hoard, J. L. *J. Am. Chem. Soc.* **1964**, *86*, 1938−1942. Hoard, J. L.; Hamor, M. J.; Hamor, T. A. *J. Am. Chem. Soc.* **1963**, *85*, 2334.
(28) Silvers, S. J.; Tulinsky, A. *J. Am. Chem. Soc.* **1967**, *89*, 3331−3337.
(29) Meyer, E. F., Jr.; Cullen, D. L. In *The Porphyrins*; Dolphin, D., Ed.; Academic Press: New York, 1978; Vol. 3, Chapter 11, pp 513−529.
(30) McCleverty, J. A. *Chem. Soc. Rev.* **1983**, *12*, 331−360.
(31) McCleverty, J. A.; Seddon, D.; Bailey, N. A.; Walker, N. W. *J. Chem. Soc., Dalton Trans.* **1976**, 898−908.

carried out on four amido[22,23,32] complexes has shown a range of 130−147° for the Mo−NH−C(1) angles, with a mean value of 137.0(16)°. The Mo−NH−C(1) angle in **3** of 141.2(14)° is close to the high end of this range. The N(O)−Mo−N(H)−C(1) torsion angle is small and is similar to values found previously.[23,32] Similar structural features are also found in the crystal structure of [5-{*o*-([Mo(NO)Tp*Cl]O)C_6H_4}-10,15,20-Ph_3porphH_2].[4]

Conclusions. The spectroscopic and electrochemical data obtained from the isomers of [5-{[Mo(NO)Tp*Cl]NHC_6H_4}-10,15,20-Ph_3porphH_2] show that, as in the related phenoxides [5-{[Mo(NO)Tp*Cl]OC_6H_4}-10,15,20-Ph_3porphH_2],[4] there is very little ground state interaction between the metal-containing redox fragment and the porphyrin redox center. However, in contrast to the structural arrangements in [5-{*o*-([Mo(NO)-Tp*Cl]O)C_6H_4}-10,15,20-Ph_3porphH_2],[4] there is not such a close approach of the pyrazolyl rings of the Tp* ligand to the porphyrin ring in **3**, all interactions being greater than 3 Å. This is also indicated by smaller anomalous shifts in the ^{1}H NMR spectrum, in particular the shifts to lower frequency of the pyrazolyl ring proton and the methyl protons in the Tp* moiety. However, it is apparent from the molecular structure of **3** and 2D-NOESY studies that the [Mo(NO)Tp*Cl] moiety is placed over the face of the ring system.

From our earlier reported photochemical studies,[5] it is evident that this class of compound undergoes photochemical excitation of the porphyrin moiety and that the observation of luminescence quenching may be associated with electron transfer to the [Mo-(NO)Tp*Cl] group. However, in contrast to the analogous phenoxides, the molybdenum centers in the amido species reduce at *ca.* −0.76 V, so that electron transfer from the excited singlet state of the porphyrin ring would seem to be thermodynamically possible only in the case of the *para* compound (Table 8). Nevertheless, the femtosecond transient absorption measurements showed that complexes **1**−**3** undergo rapid electron transfer from the excited singlet state of the porphyrin to the [Mo(NO)Tp*Cl] acceptor moiety.

Acknowledgment. We are grateful to the former SERC, now the EPSRC (N.M.R., S.S.K., T.M.F., N.T.H.W., N.N.P.), Urenco (T.M.F.), the Royal Society (G.S.B.), and the Wolfson (Scotland) Trust (E.J.L.M.) for support of this work, the Politechnika Krakowska for a leave of absence (S.S.K.), and Mr. T. Green for technical assistance.

Supporting Information Available: Full listings of H atom coordinates, bond distances and angles, and anisotropic thermal parameters for **3** (9 pages). Ordering information is given on any current masthead page.

IC9509342

(32) Al Obaidi, N.; Hamor, T. A.; Jones, C. J.; McCleverty J. A.; Paxton, K. *J. Chem. Soc., Dalton Trans.* **1986**, 1525−1530.